Direct Lattice Shaking of Bose Condensates: Finite Momentum Superfluids

Brandon M. Anderson, Logan W. Clark, Jennifer Crawford, Andreas Glatz, Igor S. Aranson, Peter Scherpelz, Lei Feng, Cheng Chin, and K. Levin

Phys. Rev. Lett. **118**, 220401 — Published 31 May 2017

DOI: 10.1103/PhysRevLett.118.220401

Direct Lattice Shaking of Bose Condensates: Finite Momentum Superfluids

Brandon M. Anderson,[1] Logan W. Clark,[1,2] Jennifer Crawford,[1] Andreas Glatz,[3,4]
Igor S Aronson,[4] Peter Scherpelz,[5] Lei Feng,[1,2] Cheng Chin,[1,2] and K. Levin[1]

[1] *James Franck Institute, University of Chicago, Chicago, Illinois 60637, USA*
[2] *Enrico Fermi Institute, University of Chicago, Chicago, Illinois 60637, USA*
[3] *Department of Physics, Northern Illinois University, DeKalb, Illinois 60115, USA.*
[4] *Materials Science Division, Argonne National Laboratory, Argonne, Illinois 60439, USA.*
[5] *Intelligence Community Postdoctoral Research Fellowship Program,*
Institute for Molecular Engineering, University of Chicago, Chicago, Illinois 60637, USA

We address band engineering in the presence of periodic driving by numerically shaking a lattice containing a bosonic condensate. By not restricting to simplified bandstructure models we are able to address arbitrary values of the shaking frequency, amplitude and interaction strengths, g. For "near resonant" shaking frequencies with moderate g, a quantum phase transition to a finite momentum superfluid is obtained with Kibble-Zurek scaling and quantitative agreement with experiment. We use this successful calibration as a platform to support a more general investigation of the interplay between (one particle) Floquet theory and the effects associated with arbitrary g. Band crossings lead to superfluid destabilization but where this occurs depends on g in a complicated fashion.

Periodic shaking of optical lattices has become an important tool for controlling and manipulating cold atom systems [1]. Shaking experiments have elucidated [2–4] quantum critical phenomena, introduced novel [5, 6] and topological [7–9] bandstructures, and addressed Kibble-Zurek (KZ) scaling [10–12]. Just as for the analogous solid state systems [13–15] the understanding of these periodically driven systems is generally based on single particle dynamics within Floquet band theory [16]. This allows the observation of dynamics in a stroboscopic but effectively time independent fashion. However, to create the novel phases suggested by the Floquet band picture turns out to be complicated [17]. Interaction effects as well as heating and dissipation arising from periodic perturbations can adversely affect this band engineering [1, 18–21].

We address these important issues in this paper using a microscopic model to directly simulate unidirectional shaking of Bose condensates. We consider a specific ("near-resonant") frequency range [2] and vary the interaction strengths, g. For g comparable to experiment [3], as was observed, we find a quantum phase transition at fixed shaking amplitude $s = s_c$ to a finite momentum superfluid state. This is associated with multiple domains having momentum $\pm q^*$. Importantly, we find quantitative agreement with these shaking experiments [3]. Armed with this support, in the more general parameter regime, we investigate heating effects. We find that Floquet band crossings are points of potential superfluid destabilization. Notably, we show where precisely this occurs is dependent on g in a very interesting way.

The quantum phase transition at s_c is addressed here and in experiment [3] using a continuous linear increase in the shaking amplitude: $s(t) = \dot{s}t$, for $t > 0$ and constant $\dot{s}$. We consider a shaking frequency slightly higher than the bandgap associated with the two lowest Bloch bands in the (static) optical lattice. At s_c, in Floquet theory the single particle dispersion $E^{\text{floq}}(k)$ transitions from having a minimum at $k = 0$ to a double well structure with minima at $k = \pm q^*$. This is illustrated in Fig. 1(a).

The number and arrangement of these $k = \pm q^*$ domains is connected to KZ theory [10–12] in a quantitative way. A scaling theory, which correlates the ramp velocity $\dot{s}$ to the distribution of topological defects (here, domain walls) was originally argued to be applicable to non-driven systems. Surprising, then is the fact that experimental observations [3] and, importantly, the present theory, show that equilibrium KZ physics seems to largely survive periodic driving. Also surprising is a second puzzle which we also address here. A driven system contains an infinitely dense set of non-adiabaticity points [22], which are potentially insurmountable and associated with Floquet band-crossings. While it is argued [22] for one body systems that these can be avoided with faster ramps, in this paper we show how many body interactions can accomplish the same thing.

There is an extensive literature on the effects of shaking of optical lattices and KZ scaling involving Bose-Einstein condensates [5, 23–30]. Also notable are many Reviews [1, 22, 31, 32] and related studies of condensate quenches [33, 34]. Accompanying this is a rather widespread theoretical literature in which condensate shaking is addressed via Bose-Hubbard models in one [20, 35, 36] or two [27] band tight-binding approximations.

In this paper we study the effects of periodic driving and many-body interactions by direct simulation of the shaken lattice. This is in contrast to previous theoretical approaches, which implement shaking on model bandstructures, and is also distinct from a periodic modulation of the lattice amplitude [37]. The dynamical bandstructure emerges naturally, through simulation of the (two dimensional) Gross-Pitaevskii equation (GPE). **Change** In this way, except for adopting the mean field GPE, our numerical scheme is general [38]. Because we

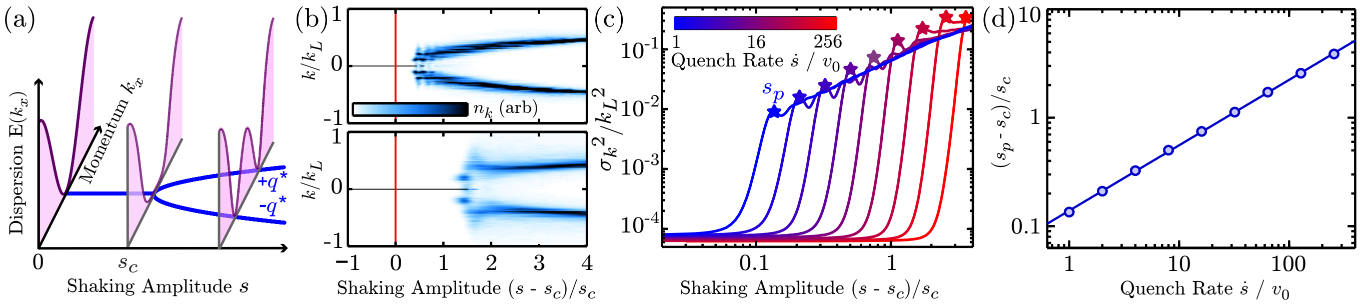

FIG. 1. Dynamics of the phase transition in a shaken optical lattice. (a) Variation in the Floquet dispersion with shaking amplitude s. At low shaking amplitudes the dispersion has a single minimum; at shaking amplitudes $s > s_c$ exceeding the critical shaking amplitude s_c, two minima appear at $\pm q^*$. (b) Bifurcation of condensate momentum-space density, $n_k(s)$ for quench rates $\dot{s} = v_3$ (top) and v_6 (bottom) where $v_n = v_0 2^n$. (c) The second moment of the momentum space dispersion for a range of ramp rates $\dot{s} = v_n$, with $n = 0 \ldots 8$. (d) The shaking amplitude at the peak (circles) scales as a power-law with the quench rate $s_p \propto \dot{s}^a$ as expected from KZ theory. A fit to this equation (solid curve) yields $a \approx 0.6$.

are not restricted to gentle shaking perturbations, we are able to address arbitrary shaking frequency, amplitude, and strength of interactions. As expected, with increasing amplitude and frequency progressively more Floquet bands (than just one or two) become relevant. As the interaction strength, g, is varied, we identify the instabilities which occur and which are found to be associated with one particle Floquet band crossings.

In this paper we address an unexplored puzzle posed by recent experiments [3]: why Kibble-Zurek theory works so remarkably well. This is all the more intriguing because the phase transition occurs in a periodically driven system. Using our simulations we attribute this to two main effects. The first is that the topological defects which are created are anomalously slow to heal. This appears to be due to their quasi-one dimensional nature. Indeed, earlier work [39, 40] has demonstrated that the healing time for 1D defects exponentially increases with the system size. The second effect has to do with understanding the criteria for superfluid breakdown due to "heating" associated with shaking. We probe this numerically by varying the interaction strength g and importantly find that choosing g to coincide with its experimental value evidently leads to an optimally stable superfluid phase.

Theoretical Approach.– We study a two-dimensional Bose condensate in a shaken optical lattice through a full microscopic simulation [38] of the Gross-Pitaevskii Equation.

$$i\hbar\partial_t \psi(\mathbf{r},t) = e^{i\gamma}\left(-\hbar^2\nabla^2/2m - \mu + V_L(x-\phi(t)) + g\,|\psi(\mathbf{r},t)|^2\right)\psi(\mathbf{r},t)\,. \quad (1)$$

where $\psi(\mathbf{r},t)$ is the condensate wavefunction at time t and position $\mathbf{r}=(x,y)$, ∇ is the gradient operator, and m is the mass of a single atom. The chemical potential μ includes zero point lattice energy ϵ_0. Here we rescale ψ at $t=0$ so that $\int|\psi(\mathbf{r},0)|^4 d\mathbf{r}/\int|\psi(\mathbf{r},0)|^2 d\mathbf{r} = 1$, and define the interaction constant $g = \mu - \epsilon_0$ corresponding to an intrinsic mean-field interaction energy. We consider a homogeneous system with periodic boundary conditions which avoids complexities associated with trapping potentials. Unless indicated otherwise, we find little significant changes [38] when we include trap effects.

The one-dimensional lattice potential $V_L(x) = U_0\sin^2(k_L x)$ has a depth U_0, lattice constant $\lambda = \pi/k_L$, and lattice recoil energy $E_L = \hbar^2 k_L^2/2m$. We choose variable interaction constant in terms of the experimental value $g_{\mathrm{expt}} \approx 0.18E_L$. Shaking is implemented through the time-dependent shift $\phi(t) = s(t)/2\sin\omega t$ of the lattice from its equilibrium value at $t=0$. We closely match experimental parameters [3] with $U_0 = 8.86E_L$, $\omega = 6.04E_L$. We chose logarithmically spaced ramp rates of the form $\dot{s} = v_0 2^n$, with $n = 0\ldots 8$ and $v_0 = 0.98\times s_c\omega/(2^8 50\pi)$; the range $n = 1\ldots 6$ then closely matches the range of experimental ramp rates [3] relevant for Figs. 2(c,d). **Change** Our GPE approach with a small phenomenological dissipation parameter $\gamma > 0$ has been applied with some success in somewhat different contexts [38, 41–44]. This is distinct from dissipation schemes [38, 45] appropriate for non-driven systems. Here we use a GPE solver based on a split-step algorithm, implemented on graphic processing units [38].

To characterize the momentum bifurcation associated with the onset of the finite-momentum condensate, we introduce the longitudinal momentum-space condensate density $n_k(t) = \int dk_y/(2\pi)|\psi(\mathbf{k},t)|^2$, where $\psi(\mathbf{k},t)$ is the momentum-space wavefunction and and we denote k_x by k. From here, we can define the second moment of the momentum-space density in the first Brillouin zone(BZ), $\sigma_k^2(t) = \int_{1\mathrm{BZ}} k^2 n_k(t)/\int_{1\mathrm{BZ}} n_k(t)$, where 1BZ is the interval $[-k_L, k_L]$ for $k_L = \pi/\lambda$. To quantify the spatial characteristics of the domain structure on length scales comparable to the lattice spacing, λ, we compute the site-averaged current-current correlation function $G_0(x) = G(x)/G(0)$, where $G(x_m) = \sum_n \int j(x_m + x_n, y)\, j(x_n, y)\, dy$ and $G(0) = \bar{j}^2$ is the

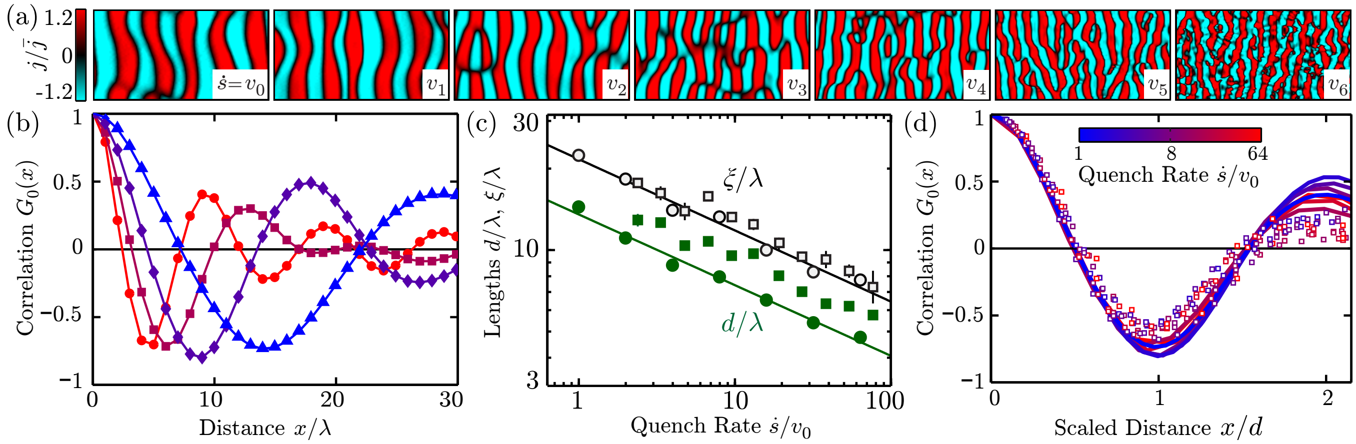

FIG. 2. Comparison of spatial structure between theory and experiment. (a) Domain structure via a snapshot of the local current density at $s = s_p$ for a range of quench rates as labelled. (b) Plots of correlation functions $G_0(x_m)$ before rescaling the distance. (c) Scaling of the typical domain size d (solid circles) and the correlation length ξ (open circles) at the shaking amplitude s_p in the numerical simulations. Both length scales follow a power law scaling: $d, \xi \propto \dot{s}^{-b}$ with $b \sim 0.26$. Experimental results for d (solid squares) and ξ (open squares) are shown for comparison [3]. (d) In scaled spatial coordinates x/d, the correlation functions for every quench rate collapse onto a single curve (solid lines), consistent with the experimental result (squares) [3].

mean-squared current.

Numerical results and analysis of GPE dynamics.– We begin by presenting results of our numerical simulation for the momentum-space condensate density $n_k(s)$, as shown in Fig. 1(b), at two different ramp rates; we henceforth express time in units of shaking amplitude through $s(t) = \dot{s}t$. For both ramp rates the condensate density is peaked at zero momentum until some time after the expected critical shaking amplitude (defined below and marked by the vertical line) is passed. Beyond this critical amplitude, the condensate bifurcates reflecting the transition in the single particle Floquet dispersion. Our numerical calculations lead to results very similar to the observations in Refs. [3]. To quantify the physics in more detail, in Fig. 1(c), we present calculations of $\sigma_k^2(s)$ for a range of ramp rates. All curves reach an equilibrium value of $\sigma_k^2(s)$ which lies on a curve consistent with an expected dependence $\sigma_k^2 \propto (q^*)^2 \propto s - s_c$.

Two key features appear as the ramp rate increases: (1) For faster ramps there is a delay in the bifurcation onset, relative to the critical point. (2) Additionally, we observe an overshoot (and sometimes a subsequent undershoot) in the curves before they settle down to the equilibrium value of $(q^*)^2$. This overshoot [46] or "ringing" effect is more apparent the faster the ramp. By studying time correlation plots from one site to another we establish that the overshoot stems from a collective oscillation of the entire condensate (and domain walls), with adjacent domains moving out of phase.

As can be seen, the most easily quantified feature of Fig. 1(c) is the amplitude, denoted s_p, of the first overshoot peak. We use this peak to characterize the temporal scaling of the bifurcation onset. It should be noted that in this one regard our analysis is different from experiment [3], as we (and experiments) find the overshoot essentially disappears for a trapped gas. In Fig. 1(d), we plot the shaking amplitude associated with the peak versus the ramp rate on a log-log plot. The clear linear dependence of this relation suggests a power law scaling, with a corresponding exponent of $a \approx 0.6$. This can be compared with the experimental exponent of $a \approx 0.5$ [3]. In this way, as in somewhat different contexts [25, 26, 47] our numerical simulations produce a KZ scaling over a large range of ramp rates.

Establishing an effective time scale variable then enables an analysis of position space scaling. Here we are able to quantitatively compare with experiment, as trapping effects appear less significant. Figure 2(a) shows sample domain configurations near a shaking amplitude s_p, for a range of ramp rates [48]. A form of self-similarity in the curves is evident with the fine domain structure shown on the right (corresponding to the most rapid ramps) and the coarser domain structure on the left (slowest ramps). This appears qualitatively consistent with the KZ picture.

For a more quantitative analysis we study the spatial correlation function $G_0(x_m)$ at s_p defined above, as shown in Fig. 2(b). The Fourier transform of this quantity has a characteristic peak k_{peak} and full-width-half-maximum, w_k, from which we define length scales $d \equiv \pi/k_{\text{peak}}$ and $\xi \equiv \pi/w_k$. These length scales are functions of $\dot{s}$ and are presented in Fig. 2(c) which shows a range of ramp rates; both scale as d, $\xi \propto \dot{s}^{-b}$ with $b \sim 0.26$. This yields quantitative agreement with experiment (shown as squares) [3]. Finally, Fig. 2(d) presents the same correlation functions in Fig. 2(b), but with the position coordinate expressed in terms of a scaled distance $d(\dot{s})$. All correlation functions lie along a universal form [49–51]. Importantly, this universal curve appears quantitatively consistent with the experimental data (shown as squares) [3].

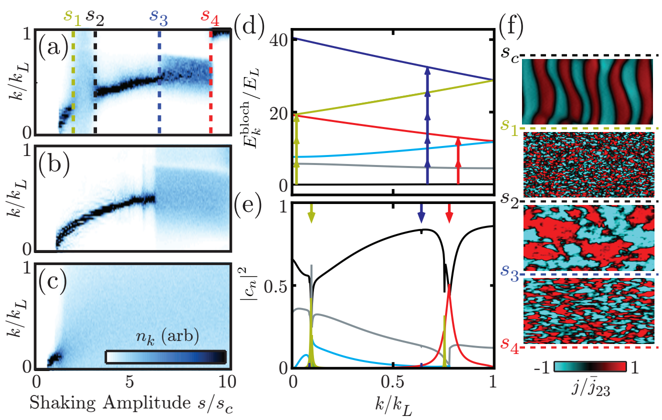

FIG. 3. Effect of interactions on Floquet evolution. Panels (a), (b), and (c), show the evolution of the condensate density in momentum-space for interaction strengths $g/g_{\rm expt} = 0.1, 1, 10$, respectively, for the quench rate $\dot{s} = v_0$. For the weakest interactions shown in panel (a), we mark the shaking amplitudes s_1 and s_3, where domains are destabilized, s_2 where domains are re-instated, and s_4 where the condensate is transferred to a single q^* superfluid without domains. (d) The lowest six Bloch bands of the unshaken lattice system, with arrows indicating resonant transitions. Each arrow has a length equal to the shaking frequency. (e) The wavefunction component of the lowest state determined from the full Floquet bandstructure calculated with fixed $s = 2.4s_c$. The colored arrows indicate the Floquet transitions that are relevant at amplitudes s_i. (f) Domain configurations for a quench with $g/g_{\rm expt} = 0.1$ taken between the marked shaking amplitudes. For reference, in units of the conventional energy scale [1, 38], $K \equiv m\omega^2\lambda(2s)$, takes the value near $s = s_c$, $K/\hbar\omega \approx 0.76$.

Instabilities associated with variable interaction strength.– When the interaction strength assumes the experimental value, $g = g_{\rm expt}$, the numerical results presented above show a consistency with experiments. We now explore the effects of variable $g/g_{\rm expt}$ ranging from 0.1, 1, and 10, as shown in Figs. 3(a), 3(b), and 3(c) respectively. We plot the momentum space condensate density $n_k(s)$ as a function of shaking amplitude, showing regions where the superfluid is destabilized. For definiteness, we take a ramp rate $\dot{s} = v_0$, about a factor of two slower than explored in experiment [3]. A dark (light), localized coloration in (a) represents a region of stable (unstable) domain formation as reflected in the current-current correlations.

Even though we vary the interaction by 2 orders of magnitude, Fig. 3 indicates that we can identify characteristic times (or equivalently shaking amplitudes) s_1 and s_3 which are evident in Fig. 3(a) and also appear either in 3(b) or 3(c). These features are points at which either the domains disappear altogether or abruptly become incoherent. One might thus expect that these robust points are intrinsic to the underlying (single particle) Floquet bandstructure and represent band-crossings as points of non-adiabaticity [22].

To address this, in Fig. 3(d) we present the six lowest Bloch bands of the unshaken, non-interacting system [38]. The counterpart plot in 3(e) represents the component c_n of the "ground-state" of the full Floquet Hamiltonain when expressed in the Bloch basis [38]. The unshaken bands in (d) are coupled in Floquet theory when the energy difference coincides with $n\hbar\omega$ [22, 52]. The figure shows resonant transitions from the first band are possible to the fourth, fifth, or sixth bands (corresponding to s_4, s_1, and s_3 respectively). These same three multi-photon transitions as in (d) can be identified in the Floquet calculation of (e) by a larger component of higher Bloch bands. Note that in the complete calculation, the resonance momenta shift slightly with s from the bare resonances in (d) [52]. What is important about this figure is that many bands are apparent, with six, six, and five bands entering in (a),(b) and (c), respectively. Only near the bifurcation point are two bands adequate for understanding the dynamics. Note also that Fig. 3(a) shows that domains are initially formed for a very short time, after which they are lost at s_1 and subsequently reformed at s_2. A small increase by a factor of three in g will reinstate domains in this intermediate region.

To summarize the key physics of (a)-(c): at weak g (and sufficiently slow ramps) one needs a small contribution from inter-boson interactions to surpass the s_1 level crossing barrier (see Figs. 3(a) and 3(b)). The presence of the very weakest magnitude interactions presumably is required for equilibration and appears to be necessary in order to form domains at all. This role of small g contrasts with the scenario in Ref. [19]. Increasing g further from Fig. 3(b) to 3(c) ultimately introduces a more turbulent behavior and undermines stability. Taking even larger g, the bifurcation disappears altogether in a rather abrupt fashion. Interestingly the optimal case, where the instabilities are maximally suppressed is for the interaction parameter $g/g_{\rm expt} = 1$.

For completeness in Fig. 3(f) we present sample domain configurations between each of the characteristic amplitudes s_i above, for $g/g_{\rm expt} = 0.1$. When the domains first appear after s_c, they are rather stripe like. After s_1, the system then loses coherent domains until they reform at s_2, but with a new correlation length along both axes. We find s_2 is not related to the Floquet resonances, but rather appears to reflect dissipation, and is highly sensitive to g. At larger s coherence is again lost at s_3. Finally, after the transition at s_4, the condensate momentum appears at the zone edge $q^* = \pm k_L$; this stable superfluid has a unique momentum component and, thus, contains no domains.

Conclusions.– In this paper we numerically addressed periodically driven systems by directly shaking (near resonance) a Bose superfluid lattice. This should be compared to one or two band Hubbard model approximations [20, 27, 35, 36] which introduce *a priori* simplifications. Our findings in Fig. 3 show, for a range of interaction strengths both large and small, that many bands tend to participate. The novel superfluid which results exhibits two types of finite- momentum domains and has features in common with a disordered form of the Larkin-Ovchinnikov-Fulde-Ferrell [53] fermionic superfluid phase.

Having these domains is particularly useful because their distribution provides a marker for visualizing distinct superfluid phases (see Fig. 3(e) and movies [48]). Moreover, the number and arrangement of domain walls is found to be quantitatively associated with KZ predictions for topological defects seen in experiment [2, 3] and in our simulations. As a highlight of this paper, we note that calibrating our numerics by first successfully addressing experiment made it possible to explore more confidently the important question of when and how the Floquet bands (of a non-interacting system) are evident in the presence of arbitrary many body interactions.

Acknowledgements.– We thank C. Parker, R. Boyack C.-T Wu for helpful conversations. This work was supported by NSF-DMR-MRSEC 1420709. The work of I.S.A. and A.G. was supported by the US Department of Energy, Office of Science, Basic Energy Sciences, Materials Science and Engineering Division. L.W.C. was supported by a Grainger Graduate Fellowship. This research was supported by an appointment (P.S.) to the Intelligence Community Postdoctoral Research Fellowship Program at The University of Chicago, administered by Oak Ridge Institute for Science and Education through an interagency agreement between the U.S. Department of Energy and the Office of the Director of National Intelligence.

[1] A. Eckardt, ArXiv e-prints (2016), arXiv:1606.08041 [cond-mat.quant-gas].
[2] C. V. Parker, L.-C. Ha, and C. Chin, Nat. Phys. **9**, 769 (2013).
[3] L. W. Clark, L. Feng, and C. Chin, Science **354**, 606 (2016), http://science.sciencemag.org/content/354/6312/606.full.pdf.
[4] A. Eckardt, C. Weiss, and M. Holthaus, Phys. Rev. Lett. **95**, 260404 (2005).
[5] M. Anquez, B. A. Robbins, H. M. Bharath, M. Boguslawski, T. M. Hoang, and M. S. Chapman, Phys. Rev. Lett. **116**, 155301 (2016).
[6] N. Goldman and J. Dalibard, Phys. Rev. X **4**, 031027 (2014).
[7] G. Jotzu, M. Messer, R. Desbuquois, M. Lebrat, T. Uehlinger, D. Greif, and T. Esslinger, Nature **515**, 237 (2014).
[8] N. Fläschner, B. S. Rem, M. Tarnowski, D. Vogel, D. S. Lühmann, K. Sengstock, and C. Weitenberg, Science **352**, 1091 (2016).
[9] J. Struck, C. Ölschläger, M. Weinberg, P. Hauke, J. Simonet, A. Eckardt, M. Lewenstein, K. Sengstock, and P. Windpassinger, Phys. Rev. Lett. **108**, 225304 (2012).
[10] T. W. B. Kibble, J. Phys. A-Math. Gen. **9**, 1387 (1976).
[11] W. H. Zurek, Nature **317**, 505 (1985).
[12] A. del Campo and W. H. Zurek, Int. J. Mod. Phys. A **29**, 1430018 (2014).
[13] T. Oka and H. Aoki, Phys. Rev. B **79**, 081406 (2009).
[14] Y. H. Yang, H. Steinberg, P. Jarillo-Herrero, and N. Gedik, Science **342**, 453 (2013).
[15] F. Mahmood, C. K. Chan, Z. Alpichshev, D. Gardner, Y. Lee, P. A. Lee, and N. Gedik, Nature Physics **12**, 306 (2016).
[16] N. Tzoar and J. I. Gersten, Phys. Rev. B **12**, 1132 (1975).
[17] A. Zenesini, H. Lignier, D. Ciampini, O. Morsch, and E. Arimondo, Phys. Rev. Lett. **102**, 100403 (2009).
[18] T. Bilitewski and N. R. Cooper, Phys. Rev. A **91**, 033601 (2015).
[19] S. Choudhury and E. J. Mueller, Phys. Rev. A **90**, 013621 (2014).
[20] S. Lellouch, M. Bukov, E. Demler, and N. Goldman, ArXiv e-prints (2016), arXiv:1610.02972 [cond-mat.quant-gas].
[21] T. Kuwahara, T. Mori, and K. Saito, Annals of Physics **367**, 96 (2016).
[22] P. Weinberg, M. Bukov, L. Alessio, A. Polkovnikov, S. Vajna, and M. Kolodrubetz, ArXiv e-prints (2016), 1606.02229 [cond-mat.quant-gas].
[23] A. Hemmerich, Phys. Rev. A **81**, 063626 (2010).
[24] M. Di Liberto, O. Tieleman, V. Branchina, and C. M. Smith, Phys. Rev. A **84**, 013607 (2011).
[25] J. Xu, S. Wu, X. Qin, Y. Ke, H. Zhong, and C. Lee, Eur. Phys. Lett. **113**, 50003 (2016).
[26] A. Russomanno and E. Dalla Torre, Eur. Phys. Lett. **115**, 30006 (2016).
[27] N. Gemelke, E. Sarajlic, Y. Bidel, S. Hong, and S. Chu, Phys. Rev. Lett. **95**, 170404 (2005).
[28] H. Lignier, C. Sias, D. Ciampini, Y. Singh, A. Zenesini, O. Morsch, and E. Arimondo, Phys. Rev. Lett. **99**, 220403 (2007).
[29] D. Chen, M. White, C. Borries, and B. DeMarco, Phys. Rev. Lett. **106**, 235304 (2011).
[30] S. Braun, M. Friesdorf, S. Hodgman, M. Schreiber, J. Ronzheimer, A. Riera, M. De Rey, I. Bloch, J. Eisert, and U. Schneider, PNAS **112**, 3641 (2015).
[31] M. Bukov, L. D'Alessio, and A. Polkovnikov, Advances in Physics **64**, 139 (2015).
[32] J. Dziarmaga, Adv. Phys. **59**, 1063 (2010).
[33] A. Polkovnikov, K. Sengupta, A. Silva, and M. Vengalattore, Rev. Mod. Phys. **83**, 863 (2011).
[34] L. E. Sadler, J. M. Higbie, S. R. Leslie, M. Vengalattore, and S.-K. D. M, Nature **443**, 312 (2006).
[35] C. E. Creffield, Phys. Rev. A **79**, 063612 (2009).
[36] M. Bukov, S. Gopalakrishnan, M. Knap, and E. Demler, Phys. Rev. Lett. **115**, 205301 (2015).
[37] C. Tozzo, M. Krämer, and F. Dalfovo, Phys. Rev. A **72**, 023613 (2005).
[38] This is discussed in more detail in the Supplementary materials.

[39] I. S. Aranson, N. B. Kopnin, and V. M. Vinokur, Phys. Rev. Lett. **83**, 2600 (1999).
[40] I. S. Aranson and L. S. Tsimring, Phys. Rev. Lett. **82**, 4643 (1999).
[41] A. Glatz, H. L. L. Roberts, I. S. Aranson, and K. Levin, Phys. Rev. B **84**, 180501 (2011).
[42] P. Scherpelz, K. Padavić, A. Rançon, A. Glatz, I. S. Aranson, and K. Levin, Phys. Rev. Lett. **113**, 125301 (2014).
[43] P. C. Hohenberg and B. I. Halperin, Rev. Mod. Phys. **49**, 435 (1977).
[44] S. Ullah and A. T. Dorsey, Phys. Rev. B **44**, 262 (1991).
[45] P. Blakie, A. Bradley, M. Davis, R. Ballagh, and C. Gardiner, Advances in Physics **57**, 363 (2008), http://dx.doi.org/10.1080/00018730802564254.
[46] I. S. Aranson, N. B. Kopnin, and V. M. Vinokur, Phys. Rev. B **63**, 184501 (2001).
[47] N. B. Kopnin and E. V. Thuneberg, Phys. Rev. Lett. **83**, 116 (1999).
[48] See http://oscon-scidac.org/projects/superfluids/shaking/ and the Supplemental Material for example videos of the growth and evolution of these domain structures as a function of time.
[49] M. Kolodrubetz, B. K. Clark, and D. A. Huse, Phys. Rev. Lett. **109**, 1 (2012), arXiv:1112.6422.
[50] A. Chandran, A. Erez, S. S. Gubser, and S. L. Sondhi, Phys. Rev. B **86**, 064304 (2012), arXiv:1202.5277.
[51] A. Francuz, J. Dziarmaga, B. Gardas, and W. H. Zurek, Phys. Rev. B **93**, 075134 (2016), arXiv:1510.06132.
[52] M. Weinberg, C. Ölschläger, C. Sträter, S. Prelle, A. Eckardt, K. Sengstock, and J. Simonet, Phys. Rev. A **92**, 043621 (2015).
[53] P. Fulde and R. A. Ferrell, Phys. Rev. **135**, A550 (1964); A. I. Larkin and Y. N. Ovchinnikov, Zh. Eksp. Teor. Fiz. **47**, 1136 (1964) [Sov. Phys. JETP **20**, 762 (1965)].